

Connections of the macaque Granular Frontal Opercular (GrFO) area: a possible neural substrate for the contribution of limbic inputs for controlling hand and face/mouth actions

Marzio Gerbella · Elena Borra · Stefano Rozzi ·
Giuseppe Luppino

Received: 24 July 2014 / Accepted: 12 September 2014 / Published online: 20 September 2014
© Springer-Verlag Berlin Heidelberg 2014

Abstract We traced the connections of the macaque Granular Frontal Opercular (GrFO) area, located in the rostralmost part of the frontal opercular margin, and compared them with those of the caudally adjacent dorsal opercular (DO) and precentral opercular (PrCO) areas. Area GrFO displays strong connections with areas DO, PrCO, and ventrolateral prefrontal (VLPF) area 12l, and even more with the mostly hand-related ventral premotor (PMv) area F5a. Other connections involve the mostly face/mouth-related PMv area F5c, the arm-related area F6/pre-SMA, the hand-related fields of VLPF areas 46v and 12r, and area SII, mostly the hand representation. Furthermore, area GrFO shows rich connectivity with several components of the limbic system including orbitofrontal areas 12o, 12m, and 11, the agranular and dysgranular insula, the agranular cingulate area 24, and the amygdala. Thalamic afferents originate primarily from the parvocellular and the magnocellular subdivisions of the mediodorsal nucleus and from midline and intralaminar nuclei. This connectivity pattern clearly distinguishes area GrFO from areas DO and PrCO, characterized by a connectivity mostly involving oral sensorimotor and gustatory areas/subcortical structures. The present data suggest, based on connectivity patterns, an involvement of area GrFO in the cortical circuits for controlling goal-directed hand and face/mouth actions. In this context, area GrFO could represent a gateway for the access of limbic

inputs, for example about subjective values, emotional significance of stimuli or internal states, to the PMv areas involved in selecting appropriate goal-directed hand and mouth/face actions.

Keywords Hand motor control · Limbic system · Gustatory cortex · Premotor cortex

Introduction

In an architectonic study of the macaque frontoparietal operculum, Roberts and Akert (1963) defined a dysgranular area lying on the opercular marginal cortex located between the anterior subcentral sulcus and the tip of the inferior arcuate sulcus and extending into the dorsal bank of the lateral fissure (LF). This area was designated as the “precentral opercular” (PrCO) area. An architectonic area, similar in location and extent to area PrCO, was defined by Barbas and Pandya (1987) and designated as area ProM.

Functional data have suggested that area PrCO is involved in gustatory functions and sensorimotor control of jaw, oropharyngeal, and laryngeal movements (Ogawa 1994; Huang et al. 1989; Jürgens and Ehrenreich 2007). In line with these data, this opercular sector appears to be connected to the primary gustatory area and to mouth-related ventral premotor (PMv) and somatosensory fields (Cipolloni and Pandya 1999).

In a recent multimodal architectonic study of the PMv (Belmalih et al. 2009), analysis of brains cut in different planes of section showed architectonic heterogeneity of the cortical sector corresponding to area PrCO (Fig. 1). Specifically, the rostralmost part of this sector appears to host an area characterized by a well-defined granular

M. Gerbella · E. Borra · S. Rozzi · G. Luppino (✉)
Dipartimento di Neuroscienze, Sezione di Fisiologia, Università
di Parma, Via Volturno 39, I-43100 Parma, Italy
e-mail: luppino@unipr.it

M. Gerbella
Brain Center for Social and Motor Cognition, Istituto Italiano di
Tecnologia (IIT), Parma, Italy

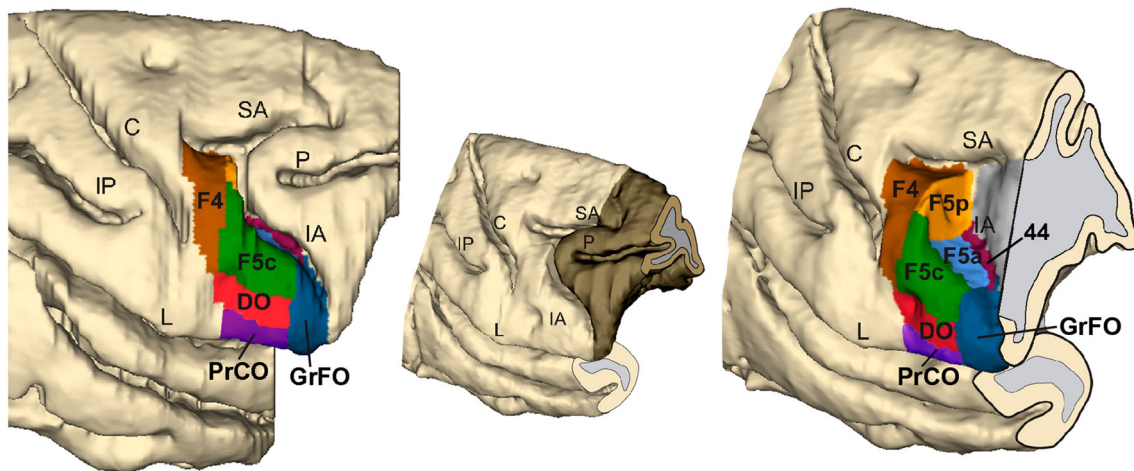


Fig. 1 Three-dimensional (3D) reconstruction of the frontal lobe of a macaque brain showing the location of the three opercular areas GrFO, PrCO, and DO and of the neighbor PMv areas. The reconstruction is shown from a dorsolateral view and from a rostralateral view in which the posterior bank of the arcuate sulcus was exposed with dissection of the 3D reconstruction along its

fundus. The brain sector removed to expose the postarcuate bank is shown with a *darker color* in the smaller 3D reconstruction shown in the middle. *C* central sulcus; *IA* inferior arcuate sulcus, *IP* intraparietal sulcus, *L* lateral fissure, *P* principal sulcus, *SA* superior arcuate sulcus

layer, originally designated as GrF (Belmalih et al. 2009) and later referred to as the “granular frontal opercular” (GrFO) area (Gerbella et al. 2011). This area borders caudally with the PMv areas F5a and F5c and with two distinct dysgranular frontal opercular areas: a more dorsal one, designated as dorsal opercular (DO) and a more ventral one for which the designation of PrCO was retained.

Recent data provided some evidence suggesting that area GrFO is distinct from the two caudally adjacent opercular areas DO and PrCO. First, though the mostly face/mouth-related ventral part of the caudal PMv area F5c is connected to these three areas, the hand- and possibly face/mouth-related rostral PMv area F5a, is connected far more strongly to area GrFO than to area PrCO and is virtually not connected with area DO (Gerbella et al. 2011). Second, functional magnetic resonance imaging data showed that grasping-related brain responses involving the two postarcuate PMv areas F5p and F5a, also extended more ventrally, toward the opercular margin, selectively in the location of area GrFO (Nelissen and Vanduffel 2011).

In the present study, to provide connective evidence for the possible distinctiveness of area GrFO and for its possible involvement in the neural circuits for organizing goal-directed hand and face/mouth actions, we examined the cortical and subcortical connections of area GrFO and compared them with those of the caudally adjacent opercular areas DO and PrCO. Preliminary data have been presented in the abstract form (Gerbella et al. 2012).

Methods

Subjects and surgical procedures

The experiments were carried out on six macaque monkeys (five *Macaca mulatta*, and one *Macaca nemestrina*) in which neural tracers were injected in area GrFO and in the two caudally adjacent opercular areas PrCO and DO. Animal handling and surgical and experimental procedures complied with the European guidelines (86/609/EEC and 2003/65/EC European Council Directives) and the Italian law in force on the care and use of laboratory animals, and were approved by the Veterinarian Animal Care and Use Committee of the University of Parma and authorized by the Italian Health Ministry.

Under general anesthesia and aseptic conditions, each animal was placed in a stereotaxic apparatus, an incision was made in the scalp, the skull trephined to remove the bone overlying the target region, and the dura opened to expose the outer portion of the frontal opercular cortex. Injection sites were chosen using cytoarchitectonic data as frame of reference (Belmalih et al. 2009), referred in terms of location of anatomical landmarks such as the arcuate sulcus, the LF, and the anterior subcentral sulcus. After the tracer injections, the dural flap was sutured, the bone replaced, and the superficial tissues sutured in layers. During surgery, hydration was maintained with saline and temperature was maintained using a heating pad. Heart rate, blood pressure, respiratory depth, and body temperature were continuously monitored. Upon recovery from anesthesia, the animals were returned to their home cages

and closely monitored. Dexamethasone and prophylactic broad-spectrum antibiotics were administered pre- and postoperatively. Analgesics were administered intra- and postoperatively.

Tracer injections and histological procedures

Once the appropriate site was chosen, the retrograde tracers Fast Blue (FB, 3 % in distilled water, Dr. Illing Plastics GmbH, Breuberg, Germany), Diamidino Yellow (DY, 2 % in 0.2 M phosphate buffer at pH 7.2, Dr. Illing Plastics) and Cholera Toxin B subunit, conjugated with Alexa 594 (CTB red, CTBr, 1 % in PBS, Invitrogen-Molecular Probes, Eugene, OR, USA), the retro-anterograde tracer Dextran conjugated with Lucifer Yellow (10000 MW, LYD, 10 % phosphate buffer 0.1 M, pH 7.4; Invitrogen-Molecular Probes), and the mostly anterograde tracer biotinylated Dextran Amine (10000 MW, BDA, 10 % phosphate buffer 0.1 M, pH 7.4; Invitrogen-Molecular Probes) were slowly pressure-injected through a glass micropipette (tip diameter 50–100 μm) attached to a 1- or 5- μl Hamilton microsyringe (Reno, NV, USA). Table 1 summarizes the locations of injections, the injected tracers, and their amounts.

After appropriate survival periods following the injections (28 days for BDA and LYD, 12–14 days for FB, DY, and CTBr), each animal was deeply anesthetized with an overdose of sodium thiopental and perfused through the left cardiac ventricle with saline, 3.5–4 % paraformaldehyde and 5 % glycerol in this order, prepared in phosphate buffer 0.1 M, pH 7.4. Each brain was then blocked coronally on a stereotaxic apparatus, removed from the skull, photographed, and placed in 10 % buffered glycerol for 3 days and 20 % buffered glycerol for 4 days. Finally, it was cut frozen in coronal sections 60- μm thick.

In all cases, one section of each five was mounted, air-dried, and quickly coverslipped for visualizing FB, DY,

and CTBr labeling in fluorescence microscopy. In Case 56l, one series of each fifth section was processed for the visualization of BDA, using a Vectastain ABC kit (incubation 60 h; Vector Laboratories, Burlingame, CA, USA) and 3,3'-diaminobenzidine (DAB) as a chromogen. The reaction product was intensified with cobalt chloride and nickel ammonium sulfate. In the same case, one series of each fifth section was processed to visualize LYD and BDA, respectively, using the double-labeling protocol described in detail in Gerbella et al. (2010). Briefly, the sections were first processed to visualize BDA, except for a shorter incubation period in ABC solution (overnight) and then BDA was stained brown using DAB. Then, the sections were incubated overnight in avidin–biotin blocking reagent (Vector SP-2001), for 72 h at 4 °C in a primary antibody solution of rabbit anti-LYD (1:3,000; Invitrogen), 0.3 % Triton, and 5 % normal goat serum in 0.01 M phosphate-buffered saline at pH 7.4, and for 1 h in biotinylated secondary antibody (1:200, Vector), 0.3 % Triton, and 5 % normal goat serum in 0.01 M phosphate-buffered saline at pH 7.4. Finally, LYD labeling was visualized using the Vectastain ABC kit (Vector Laboratories) and the Vector SG peroxidase substrate kit (SK-4700, Vector) as a chromogen. With this procedure, BDA labeling was stained brown and the LYD labeling was stained blue in the same tissue sections. In all cases, one series of each fifth section was stained with the Nissl method (thionin, 0.1 % in 0.1 M acetate buffer, pH 3.7).

Data analysis

The criteria used for the definition of the FB, DY, CTBr, BDA, and LYD injection sites and labeling have been described in earlier studies (Luppino et al. 2003; Rozzi et al. 2006; Gerbella et al. 2011). The injection sites were attributed to the various areas under study using previously described cytoarchitectonic criteria (Belmalih et al. 2009). All the injection sites presented in this study were confined to the cortical gray matter and to a single architectonic area.

The distribution of retrograde (for all tracer injections, but BDA) and anterograde (for BDA and LYD injections) cortical labeling was analyzed in sections every 300 μm and plotted in sections every 600 μm , together with the outer and inner cortical borders, using a computer-based charting system. The distribution of the labeling in the LF was visualized in 2D reconstructions obtained using the same software, as follows (for more details, see Matelli et al. 1998). In each plotted section, the cortical region of interest was subdivided into columnar bins by lines perpendicular to the cortical surface, connecting the outer and inner cortical contours. The cortex was then unfolded at the level of a virtual line connecting the midpoints of all the

Table 1 Monkey species, localization of the injection sites, and tracers employed in the experiments

Monkey	Species (<i>Macaca</i>)	Left/right	Area	Tracer (%)	Amount
Case 33	<i>nemestrina</i>	L	DO	CTBr 1	1 × 1 μl
Case 42	<i>mulatta</i>	R	DO	FB 3	1 × 0.2 μl
Case 44	<i>mulatta</i>	L	GrFO	CTBr 1	1 × 1 μl
Case 54	<i>mulatta</i>	L	PrCO	FB 3	1 × 0.2 μl
Case 56	<i>mulatta</i>	L	GrFO	BDA 10	2 × 1 μl
		L	GrFO	LYD 10	1 × 1.3 μl
		R	GrFO	FB 3	1 × 0.2 μl
		R	PrCO	DY 2	1 × 0.2 μl
Case 61	<i>mulatta</i>	R	GrFO	FB 3	1 × 0.2 μl

perpendicular lines, approximately positioned at the border between layers III and IV. The unfolded sections were then aligned to correspond with the fundus of the upper bank of the LF and the labeling distributed along the space between two consecutive plotted sections (600 μm).

Data from individual sections were also imported into a 3D reconstruction software package (Bettio et al. 2001). The distribution of the cortical labeling on the exposed cortical surfaces was visualized in dorsolateral, mesial, and bottom views of the 3D reconstructions of the hemispheres. The distribution of the labeling along the postarcuate bank was visualized in non-standard views of the hemispheres in which the bank was exposed by appropriate dissections of the 3D reconstructions (Rozzi et al. 2006).

The criteria and maps used for the areal attribution of the labeling were mostly similar to those used in a previous study (Gerbella et al. 2011). The attribution of the labeling to agranular frontal and cingulate areas was made according to architectonic criteria described by Matelli et al. (1985, 1991) and Belmalih et al. (2009). The ventrolateral prefrontal (VLPF), the orbitofrontal, and the rostral insular cortex were subdivided according to architectonic criteria described by Carmichael and Price (1994). In the parietal operculum, we matched our data with functional maps of the SII region defined by Fitzgerald et al. (2004).

In all cases of retrograde tracer injections, we counted the number of cortical-labeled neurons plotted in the ipsilateral hemisphere in sections at every 600- μm interval beyond the limits of each injected area. Then, cortical afferents to different injected areas were expressed in terms of the percent of labeled neurons found in a given cortical area or sector, with respect to the overall labeling. Furthermore, after injections in area GrFO, the labeling attributed to a given area and reliably observed across different sections and cases was analyzed in sections at every 300 μm in terms of the following: (1) percentage of retrogradely labeled neurons located in the superficial (II–III) versus deep (V–VI) layers (s/d ratio), and (2) laminar distribution of the anterogradely labeled terminals (for the BDA and the LYD injections).

The distribution of the retrograde labeling in the thalamus and in the amygdalar complex was analyzed in all the cases of fluorescent tracer injections except for the CTBr thalamic labeling, as intense red autofluorescence in some thalamic nuclei prevented reliable identification of labeled cells. Thalamic- and amygdalar-labeled cells were plotted in sections every 300 μm , together with the outline of the ventricles and of blood vessels, using a computer-based charting system. The borders of thalamic and amygdalar nuclei/subnuclei, defined in adjacent Nissl-stained sections, were then superimposed with a microprojector on the plots of labeled cells using the outline of the ventricles and of blood vessels. The relative contribution of inputs from different thalamic

nuclei to the areas under study was expressed in terms of percent of labeled neurons found in a given thalamic nucleus, with respect to the total number of thalamic-labeled cells plotted in sections at every 300- μm interval.

The borders of the thalamic nuclei were primarily defined according to the cytoarchitectonic criteria and the nomenclature used by Olszewski (1952), and the amygdalar complex was subdivided according to the criteria described by Amaral et al. (2003).

Results

Cytoarchitecture of the rostral opercular frontal cortex and location of the injection sites

Architectonic features, location, and extent of area GrFO have been already described by Belmalih et al. (2009) and will be briefly recalled here. Area GrFO is located in the rostralmost part of the frontal opercular cortex, extending from the ventralmost part of the inferior arcuate sulcus to the outermost part of the orbitofrontal surface (Fig. 1). In the standard coronal plane, this cortical sector is typically cut more or less tangentially to the cortical surface making its architecture sometimes difficult to delineate. Optimal views of the architectonic features of area GrFO can be obtained in non-standard planes of section, such as tangential to the arcuate sulcus sections (Fig. 2a). The distinguishing cytoarchitectonic features of this area are an evident layer IV and a relatively dense layer V, populated by densely packed, small pyramids (Fig. 2b). Layer III is relatively homogeneous in cell and size density and layer VI is sublaminate. The presence of an evident layer IV is an architectonic feature very useful for delineating this area even in coronal sections (Fig. 3a, b). In the posterior bank of the arcuate sulcus, area GrFO borders caudally with the PMv area F5a (Fig. 2a). The absence of an even faint layer IV and the presence of deeply stained, relatively large pyramids in the lowest part of layer III (Fig. 2c) distinguish F5a from GrFO. In the postarcuate convexity cortex, area GrFO borders caudally with the PMv area F5c, an agranular area characterized by a very poorly laminated appearance (Belmalih et al. 2009). More ventrally, on the opercular margin, GrFO borders caudally with two dysgranular areas: DO and PrCO. In area DO (Fig. 2d), granular cells are very few, intermingled with layers III and V pyramids, and layer V is relatively prominent. In area PrCO, a faint layer IV is discernable and layer V is denser than in area DO. Decrease in myelin content and increase in SMI-32 immunopositive layer III pyramids were also found to further distinguish PrCO from DO (Belmalih et al. 2009). In the outermost part of the orbital surface, area GrFO borders with orbitofrontal area 12o, which can be distinguished for

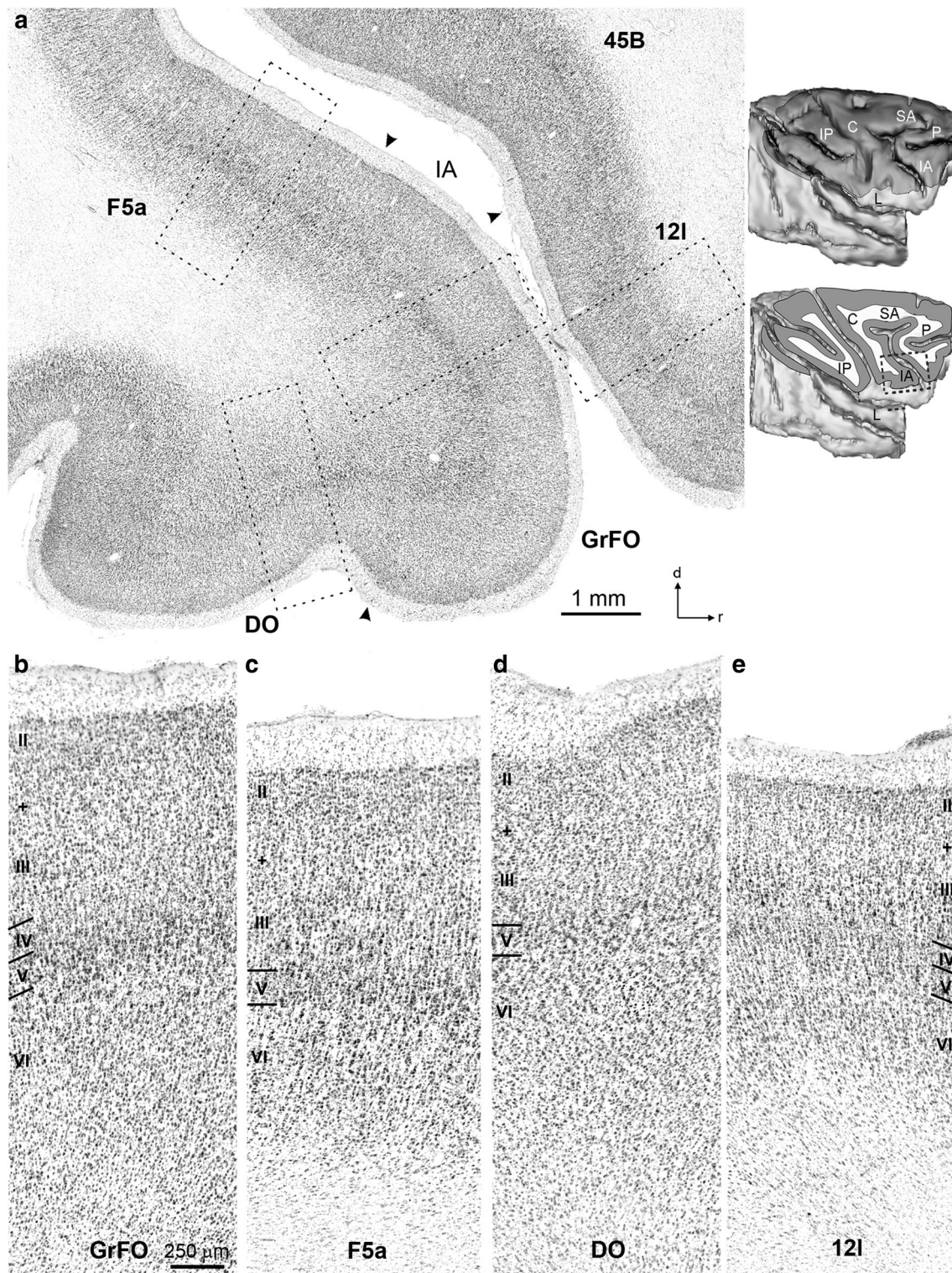


Fig. 2 **a** Low-power photomicrograph of a Nissl-stained section cut tangential to the arcuate sulcus, from a celloidin-embedded hemisphere. On the *right*, the dark gray region of the upper 3D reconstruction of the brain shows the sector removed to expose the plane of the section on the lower 3D reconstruction. The dashed box on the lower 3D reconstruction delineates the location of the

photomicrograph. *Arrowheads* on the photomicrograph indicate the borders between cytoarchitectonic areas, and the *dashed boxes* mark the location of the higher magnification views in **b** (GrFO), **c** (F5a), **d** (DO), and **e** (12I). All the sections and reconstructions in this and in the subsequent figures are shown as right hemispheres. *d* dorsal, *r* rostral, other abbreviations as in Fig. 1. *Scale bar* in **b** applies to **b–e**

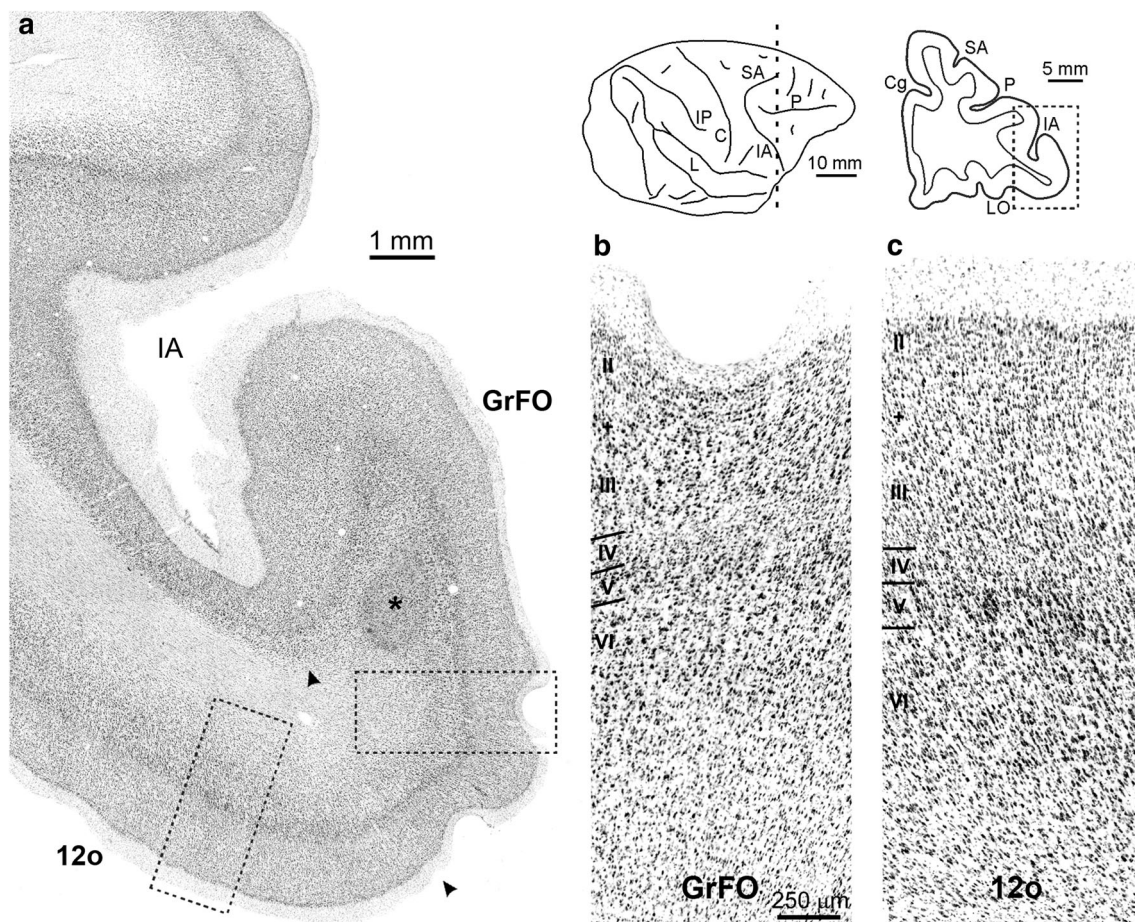


Fig. 3 **a** Low-power photomicrograph of a Nissl-stained coronal section taken from Case 441. The *asterisk* indicates the location of the CTBr injection site. The level at which the section was taken is indicated by a *dashed line* on the drawing of the dorsolateral view of the hemisphere. The *dashed box* in the section drawing indicates the location of the photomicrograph. *Dashed boxes* * **a** indicate the

location of the higher magnification views in **b** (GrFO), **c** (12o). Abbreviations as in Fig. 1. *Scale bar* in **b** applies to **b**, **c**. Note that apparent differences in cell size and density between the section shown in this figure and that shown in Fig. 2 can be accounted for by differences in shrinkage due to different histological processing

a less sharply defined layer IV, a less prominent layer V, and a homogeneous layer VI (Fig. 3c). Rostrally, area GrFO borders with the ventrolateral prefrontal area 12l, characterized by an evident size gradient in layer III, a well-developed layer IV, and a sublaminated layer V (Fig. 2e).

In area GrFO, the five tracer injections were located at different dorsoventral levels all together likely involving almost the entire extent this area (Fig. 4). In area DO, the two tracer injections were located one more rostrally, the other more caudally. Finally, in area PrCO, the two tracer injections were located just caudal to the border with area GrFO.

Cortico-cortical connections of area GrFO

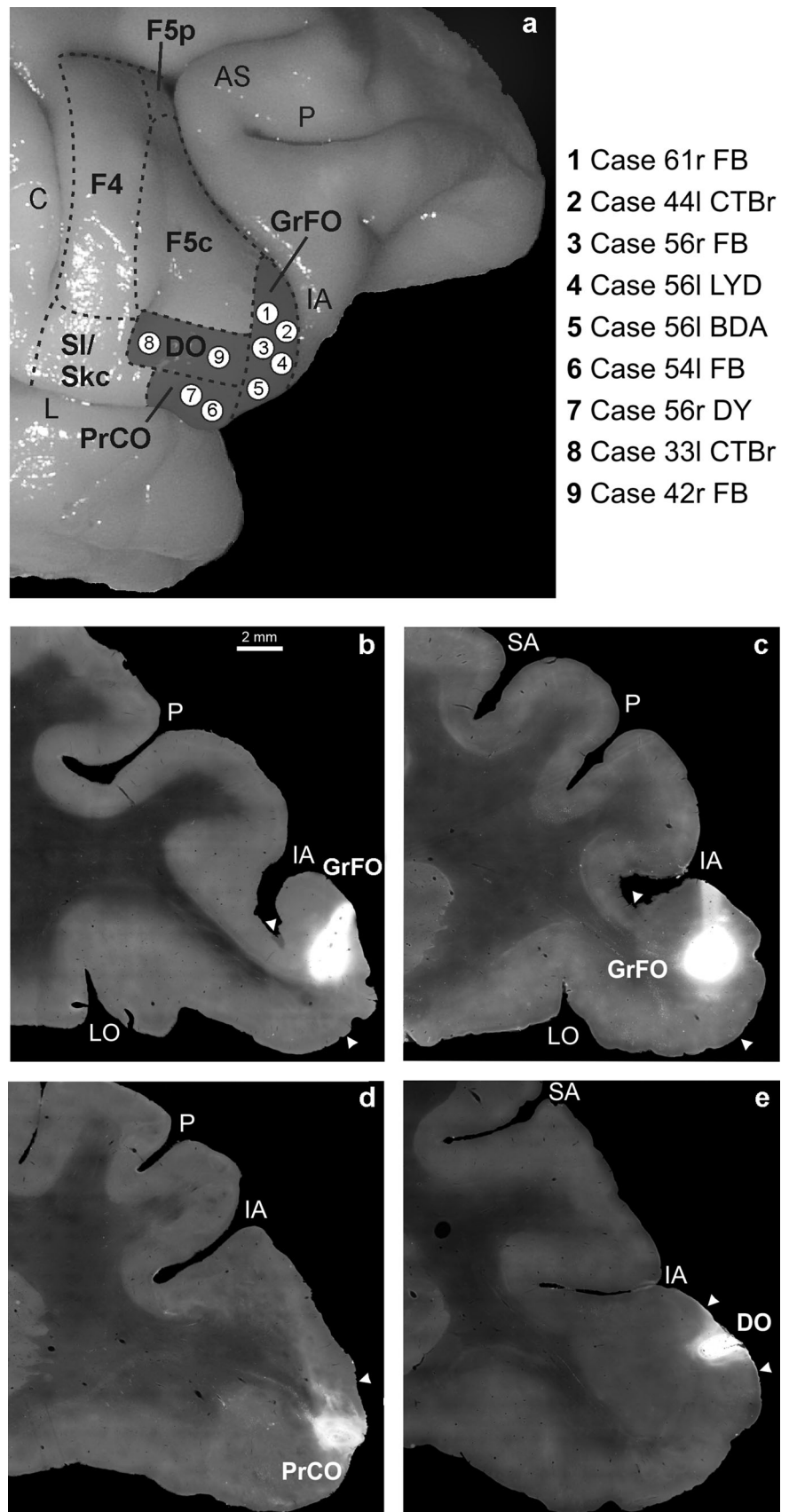
Five tracer injections placed in area GrFO displayed a connectivity pattern quite consistent across different cases.

The distribution of the retrograde labeling observed in Cases 441 CTBr and 61r FB and the anterograde labeling observed in Case 56l BDA is shown in Figs. 5 and 6. Table 2 shows the percent distribution of the retrograde labeling observed in the three cases of fluorescent tracer injections.

In all the cases, the labeling extended caudally to area GrFO involving very densely both areas DO and PrCO (Figs. 5, 6e, e'). The labeling also extended in the PMv, where it was very rich in the mostly hand-related area F5a, also involving the adjacent fundal area 44 and considerably weaker in the mostly face/mouth-related ventral part of area F5c (Figs. 5, 6e, f, e'). Some labeling, especially in Case 441 CTBr, was observed in area F6/pre-SMA (Figs. 5, 6d, f, f'). Relatively dense labeling also involved different subdivisions of the agranular cingulate area 24 (Fig. 6d, f, d', f'). The labeling was located either on the cingulate gyrus (areas 24a and 24b) or in the

Fig. 4 Injection sites in areas GrFO, PrCO, and DO.

a Composite view of all the injection sites, shown as white circles, mapped on a template hemisphere. *Dashed lines* mark cytoarchitectonic borders of the opercular areas, shaded in *gray*, and their neighbors. **b** CTBr injection site in area GrFO in Case 44l; **c** FB injection site in area GrFO in Case 61r; **d** FB injection site in area PrCO in case 54l; **e** FB injection site in area DO in Case 42r. *Scale bars* in **b** applies to **b–e**. *LO* lateral orbital sulcus. Other abbreviations as in Fig. 1



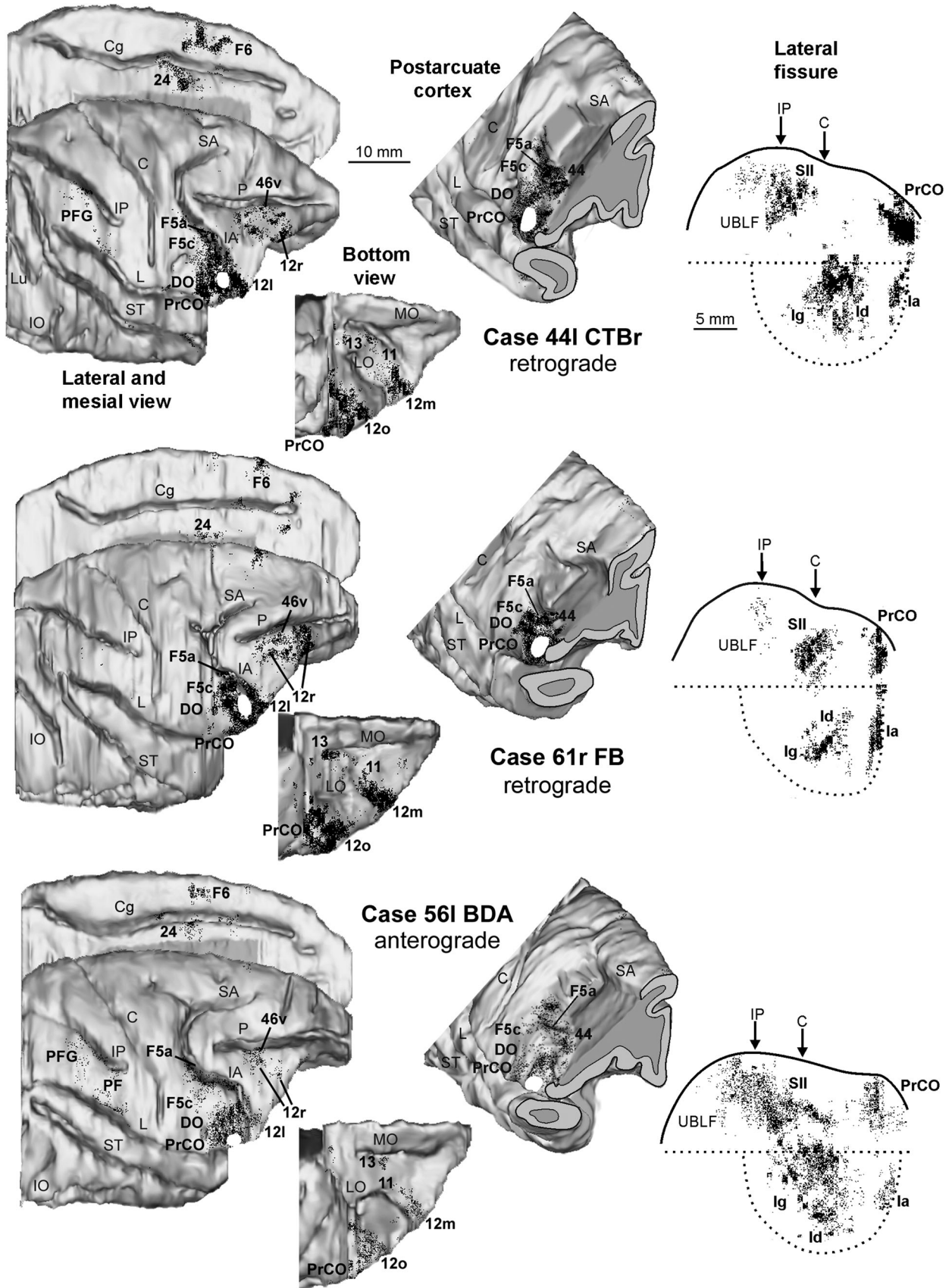


Fig. 5 Distribution of the retrograde (Cases 44l CTBr and 61r FB) and anterograde (Case 56l BDA) labeling observed after injections in area GrFO. The labeling is shown in dorsolateral, medial, and bottom views of the 3D reconstructions of the injected hemispheres, in non-standard views of 3D reconstructions of the postarcuate cortex, shown as in Fig. 1, and in 2D reconstructions of the LF. For the retrograde labeling, each *dot* corresponds to one labeled neuron, and for the anterograde labeling, the *dot* density is proportional to the density of the observed labeled terminals (one *dot* is equivalent to about 15–25 labeled terminals). Each 2D reconstruction of the LF was aligned to correspond with the dorsal border of the insula indicated by a *straight dotted line*; the *continuous line* marks the lip of the bank, and the *curved dotted line* marks the border of the insula with the lower bank of the sulcus. *Arrows* mark the levels of the rostral tip of the intraparietal sulcus (IP) and of the rostralmost level of the central sulcus (C). The location of each tracer injection is shown as a white area on the dorsolateral view of the hemisphere. *Cg* cingulate sulcus, *IO* inferior occipital sulcus, *Lu* lunate sulcus, *MO* medial orbital sulcus, *ST* superior temporal sulcus, *UBLF* upper bank of the LF. Other abbreviations as in Fig. 1

cingulate sulcus in the cingulate motor areas 24c and 24d, especially in Case 56r FB. In the prefrontal cortex, there were several relatively richly labeled VLPF and orbitofrontal areas, especially in Case 61r FB. Specifically, dense labeling was observed in the VLPF area 12l, just rostral to area GrFO (Figs. 5, 6c, c'). More rostrally, marked cells and terminals were observed in the two hand-related VLPF fields rostral 46vc and intermediate 12r (Fig. 6a–c, b', c'; Borra et al. 2011; Gerbella et al. 2013). In the orbitofrontal cortex, quite rich labeling was observed in area 12o and, more rostrally, in areas 11 and 12m (Fig. 6a, b, d, a', d'). Labeled cells and terminals were also observed in area 13, especially in Case 61r FB. Very rich labeling was also observed in two distinct zones of the insular cortex. One was located more rostrally in the agranular insula, the other more caudally, mostly involving the dysgranular insula (Figs. 5, 6e–g, e'–g'). Marked cells and terminals were observed also in the upper bank of the LF in the location of area SII (Figs. 5, 6g, h, g', h'). In Cases 61r FB and 44l CTBr, the labeling appeared to be more concentrated in a more rostral and a more caudal zone, respectively. In Case 56l BDA, both zones were involved by the anterograde labeling. Comparison with functional studies of the SII region (Fitzgerald et al. 2004) suggests that the labeling altogether involved mostly the SII digit representation, but could also extend more rostrally in the SII mouth representation. Finally, very sparse labeling was found in rostral inferior parietal areas PF, PFG and AIP.

In all cases of retrograde tracer injections, labeled cells in almost all the connected areas were almost equally distributed in the supra- vs. infragranular cortical layers (Fig. 7a'–d') and the anterograde labeling tended to be relatively evenly distributed across all cortical layers (Fig. 7a–d) suggesting connections of the “lateral” type

(Felleman and Van Essen 1991). In area SII (Fig. 7e, e'), the proportion of labeled cells found in the supra- vs. infragranular cortical layers was >66 %, and the anterograde labeling tended to involve all layers except layer IV. According to Felleman and Van Essen (1991), this pattern suggests that, based on the distribution of the retrograde labeling, SII send feedforward projections to GrFO and, based on the distribution of the anterograde labeling, GrFO sends feedback projections to SII.

Cortical connections of areas PrCO and DO

As the aim of the tracer injections in area PrCO was to compare the connectivity of this area with that of area GrFO, the injection sites in Cases 54l FB and 56r DY were placed in the convexity cortex caudal to area GrFO. Accordingly, these data could only partially describe the connectivity pattern of this area, which also extends in the dorsal bank of the LF. However, the connectivity pattern observed in the two cases, shown for Case 54l FB in Fig. 8 and for both cases in Table 2, was remarkably similar and quite different from that of area GrFO.

In the frontal opercular cortex (Fig. 8b–f), dense labeling extended from area PrCO to the adjacent areas DO and GrFO. Furthermore, very dense labeling was located caudal to area PrCO in the opercular part of the somatic koniocortex (Skc; Roberts and Akert 1963; Jones and Burton 1976). Dense labeling was also observed in the fundus of the superior limiting sulcus, in the location of the primary gustatory area (area G, Carmichael and Price 1994). Both Skc and area G were virtually not connected to area GrFO. No labeling was observed in the location of area SII. In the PMv, differently from area GrFO, area PrCO appeared to be much more densely connected to area F5c than to area F5a (Fig. 8c, d). In the prefrontal cortex, marked cells were relatively rich in area 12l and relatively poor in area 46v. In the orbitofrontal cortex, some labeling was observed in areas 11, 12o, and 13 (Fig. 8a, b). Finally, very dense labeling was observed in the insular cortex, most of it in the agranular insula.

A further distinct connectivity pattern was observed after the two tracer injections in area DO, illustrated for Case 42r FB in Fig. 9 and for both cases in Table 2. One distinguishing feature observed in both the cases was a connectivity pattern mostly confined to the surrounding areas/fields. Specifically, most of the labeling was located in the adjacent areas GrFO, PrCO, and Skc (Fig. 9a–f). The labeling also involved the agranular insula. In the PMv, the labeling was very dense in area F5c and virtually absent in area F5a. Furthermore, very dense labeling was located in the lateral part of the caudal PMv area F4 (Fig. 9e, f), where mouth movements are mostly represented (Gentilucci et al. 1988; Huang et al. 1989; Maranesi et al. 2012).

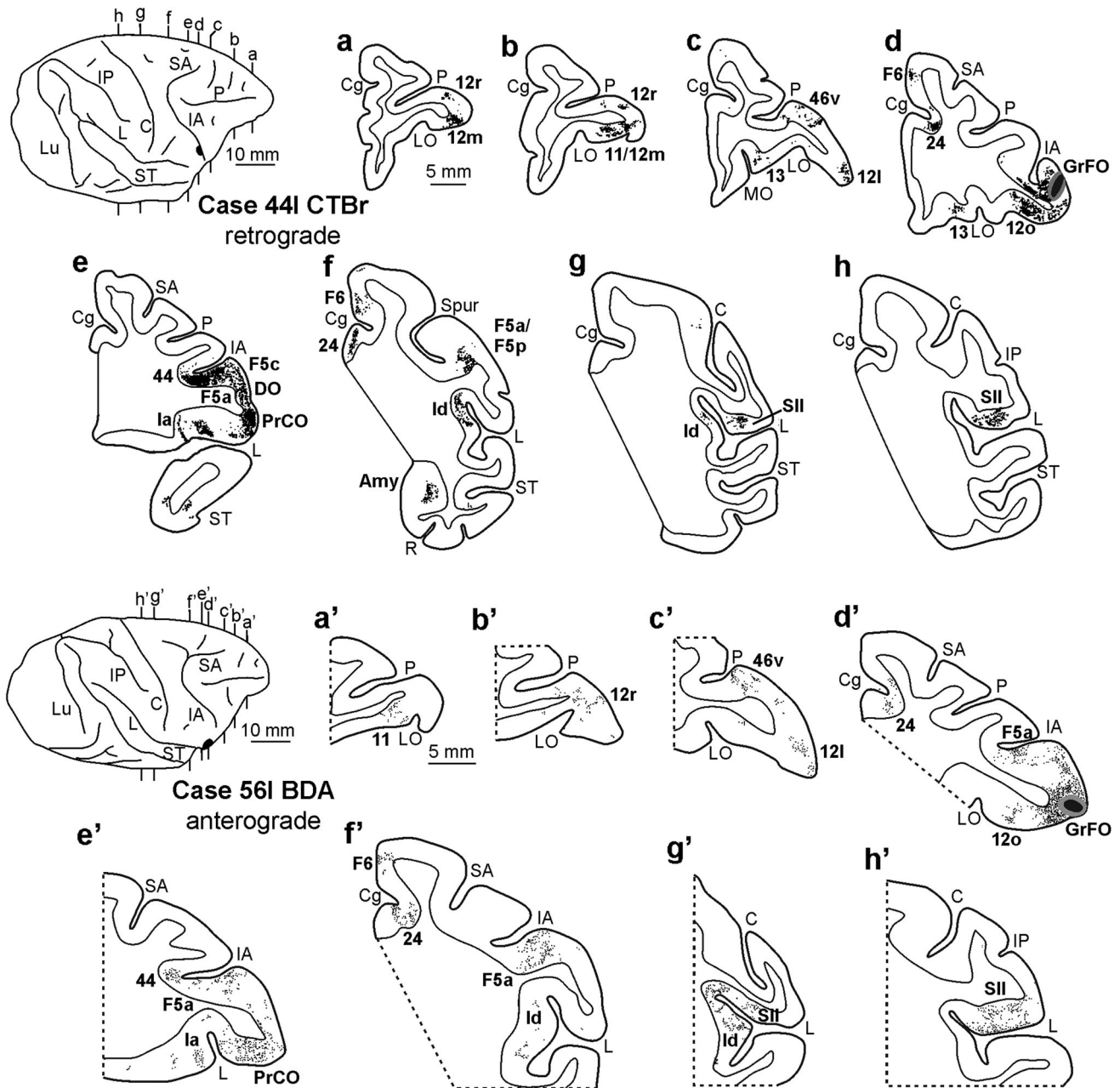


Fig. 6 Distribution of the retrograde (*upper part*) and of the anterograde (*lower part*) labeling observed in Cases 44I CTBr and 56I BDA, respectively, shown in drawings of representative coronal sections. Sections are shown in a rostral to caudal order (**a–h** and **a'–h'**). The injection sites are shown as a *black zone* corresponding to

the core, surrounded by a *gray zone* corresponding to the halo. For each case, a dorsolateral view of the injected hemisphere shows the levels at which the sections were taken and the location of the injection site. Other abbreviations and conventions as in Figs. 1, 4 and 5

Thalamic and amygdalar inputs to areas GrFO, PrCO, and DO

The distribution of the thalamic labeling observed after tracer injections in areas GrFO, PrCO, and DO is illustrated in Fig. 10 and Table 3. After the two FB injections in area GrFO in Cases 56r and 61r, the highest proportion of labeled cells was located in the ventral part the mediadorsal (MD)

nucleus, along its almost entire rostrocaudal extent. The majority of these cells was located in the parvocellular (MDpc) subdivision. However, a relatively high proportion of labeling was also observed in the magnocellular (MDmc) subdivision. A relatively high number of labeled cells was also observed in the motor thalamus, mostly involving the parvocellular ventral anterior (VApc) and the medial ventral lateral (VLM) nuclei and, to a lesser extent, the middle of

Table 2 Percent distribution (%), mean percent values (in bold), and total number (*n*) of cortical-labeled neurons observed following retrograde tracer injections in GrFO, PrCO, and DO

Injected area	GrFO				PrCO			DO		
	C44l CTBr (%)	C56r FB (%)	C61r FB (%)	Mean (%)	C54l FB (%)	C56r DY (%)	Mean (%)	C33l CTBr (%)	C42r FB (%)	Mean (%)
Orbitofrontal										
12m/11	3.7	6.8	9.2	6.5	1.3	2.7	2	*	*	*
12o	7.7	6.1	9.9	7.9	1.9	1.6	1.7	–	–	–
13	1	*	2.8	1.3	2.3	*	1.4	–	–	–
Total orbitofrontal	12.4	13	21.9	15.7	5.5	4.8	5.1	*	*	*
VLPF										
12r	2.6	2.1	7.1	3.9	*	*	*	*	1	*
46v	1.9	3	4.8	3.2	1.1	*	*	–	–	–
12l	5.5	8.2	6.6	6.8	5.8	2.9	4.3	–	–	–
Total VLPF	10	13.3	18.5	13.9	6.9	3	4.9	*	1	*
Opercular										
GrFO	/	/	/	/	18.1	14.2	16.1	21.4	20.4	20.9
PrCO	10.8	7.8	7.7	8.8	/	/	/	26	24.2	25.1
DO	6.2	10	6.8	7.7	11.6	13.8	12.7	/	/	/
G	–	*	*	*	6.7	11.9	9.3	–	1	*
Total opercular	17	17.8	14.5	16.5	36.2	39.9	38	47.4	45.6	46.5
Insular cortex										
Agranular	5	8.9	6.4	6.8	14.6	22.2	18.4	*	5.2	3
Dysgranular/granular	12.6	11.4	6.2	10.1	9.2	5.7	7.4	*	2	1.4
Total insular cortex	17.6	20.3	12.6	16.9	23.8	27.9	25.8	1.6	7.2	4.4
Premotor										
F5a/44	22.7	15	17.5	18.4	2.2	2.4	2.3	*	*	*
F5c	1.5	2.4	3.4	2.4	9	5.9	7.4	10.5	8.8	9.6
F4	–	*	–	*	–	–	–	16.7	16.4	16.6
F6/pre-SMA	4.1	1.2	1.2	2.2	–	–	–	–	*	*
Total premotor	28.9	18.6	22.1	23.1	11.2	8.3	9.7	27.4	26.3	26.8
Somatosensory										
SI/Skc	–	*	–	*	14	15.4	14.7	23.1	17.5	20.3
SII	6.3	3	2.6	3.9	*	*	*	*	*	*
Total somatosensory	6.3	3.1	2.6	4	14.5	15.9	15.2	23.5	18.1	20.8
Cingulate cortex										
24a/24b	1.9	3.5	2.1	2.5	–	–	–	–	–	–
24c/24d	4	8	3.7	5.2	1.4	*	*	*	1.6	*
Total cingulate	5.9	11.5	5.8	7.7	1.4	*	*	*	1.6	*
Others	2.5	1.2	1.5	1.7	*	*	*	–	*	*
Total number ^a	31543	22604	25108		13428	10256		9883	24072	

/ Injected area, – No labeling, * Labeling <1 %

^a Total number of cortical-labeled neurons plotted in the ipsilateral hemisphere in sections at every 600- μ m interval beyond the limits of each injected area

area X. Finally, a very high proportion of labeled cells was observed in intralaminar and, even more, in midline thalamic nuclei, especially in Case 61r.

Different profiles of thalamic afferents were observed after the tracer injections in areas PrCO and DO. Specifically, after the FB and the DY injections in area PrCO in

Cases 54l and 56r, respectively, the highest proportion of labeled cells, as for area GrFO, was found in the ventral part of MD nucleus. However, the labeled zone was located in the caudal two-thirds of the MD and was almost entirely confined to the MDpc. In the motor thalamus, the proportion of labeled cells in VApC and VLm was much weaker

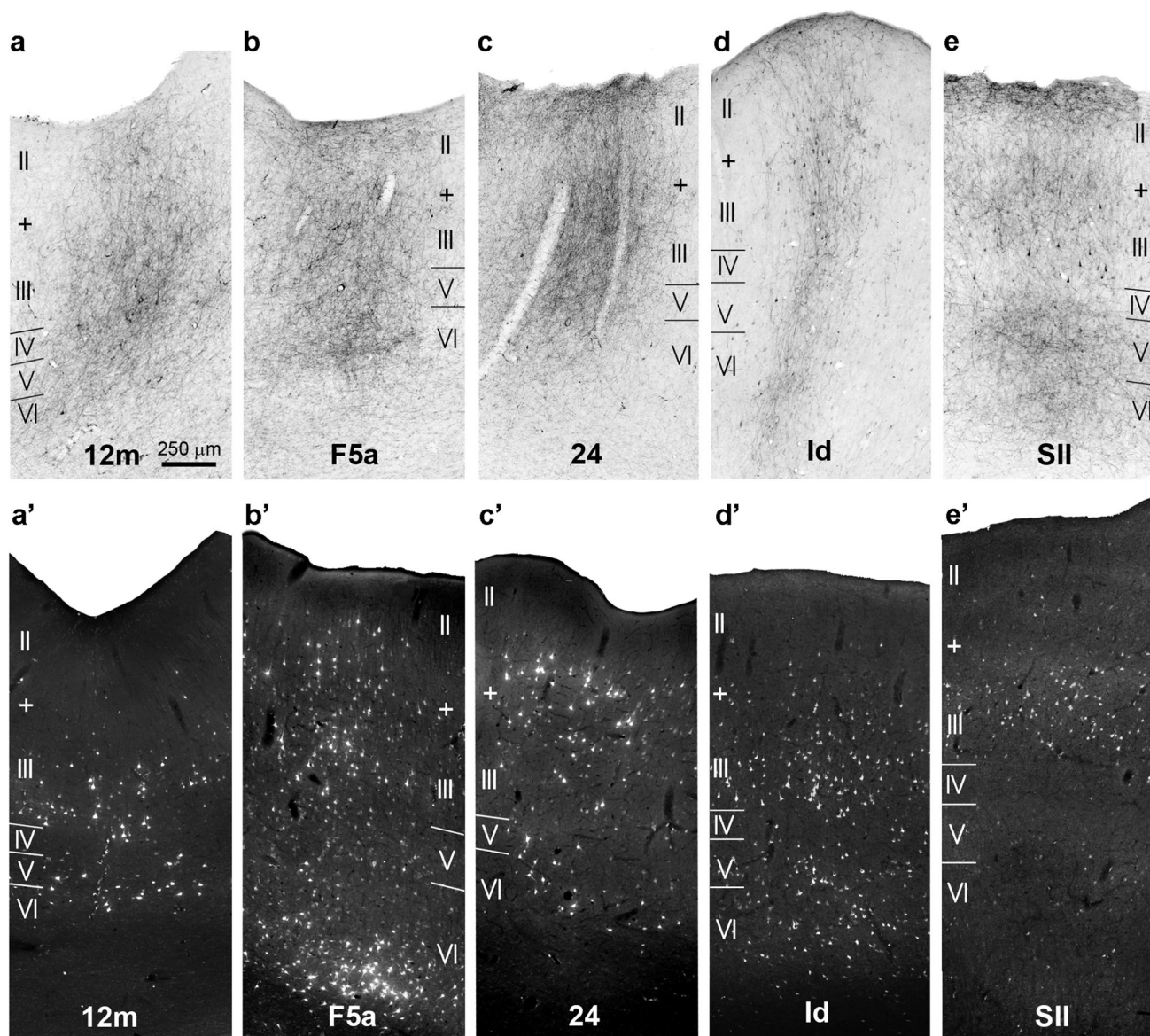


Fig. 7 Laminar patterns of anterograde and retrograde labeling observed following injections in area GrFO. The cortical location of each photomicrograph is indicated for Case 561 LYD (**a–c**), Case 561

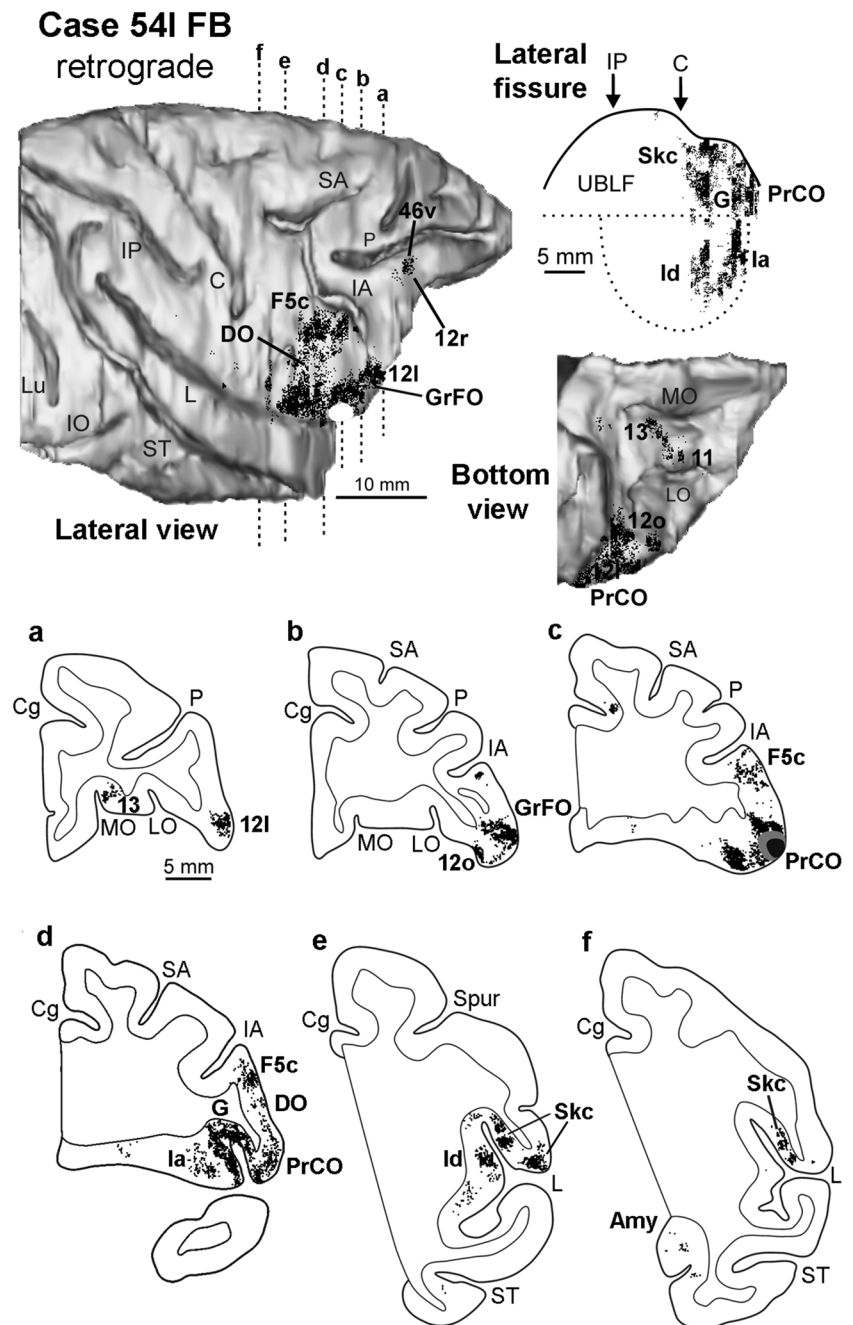
BDA (**d, e**), Case 61r FB (**a', b'**), Case 56r FB (**c'**), and Case 441 CTBr (**d', e'**). Scale bar in **a** applies to all photomicrographs

than that observed for area GrFO. Furthermore, a relatively high proportion of labeled cells was observed in the ventral posteromedial (VPM) nucleus and, even more, in its parvocellular (VPMpc) subdivision. In both cases, but especially in Case 54l FB, rich labeling was observed in the centromedian, the parafascicular, and in the midline thalamic nuclei. After the tracer injection in area DO (Case 42r FB) again the highest proportion of labeled cells was located in MDpc. Their distribution was similar to that observed for area PrCO. A relatively high proportion of the labeling was located in the motor thalamic nuclei VApC and VLm and even more in the ventrolateral part of area X. Few marked cells were observed in VPMpc. As for area

PrCO, rich labeling was observed in intralaminar and midline thalamic nuclei.

A further major source of subcortical projections to area GrFO was the amygdalar complex. Specifically, in all the three cases of fluorescent tracer injections, numerous labeled cells were observed mostly in the rostral half of the basal (B) nucleus. The labeling mostly involved the intermediate (Bi) subdivision, but also extended in the parvocellular (Bpc) subdivision (Fig. 11). Qualitative analysis carried out in Cases 561 LYD and BDA showed that the amygdala was devoid of labeled terminals. Labeled cells in the rostral part of the B nucleus were also observed after tracer injections in area PrCO in Cases 54l FB and 56r DY.

Fig. 8 Distribution of the retrograde labeling observed after injections in area PrCO in Case 54l FB, shown in dorsolateral and bottom views of the 3D reconstructions of the injected hemisphere and in a 2D reconstruction of the LF (*upper part*), and in drawings of coronal sections arranged in a rostral to caudal order (*a–f lower part*). Abbreviations and conventions as in Figs. 1, 4, 5, and 6



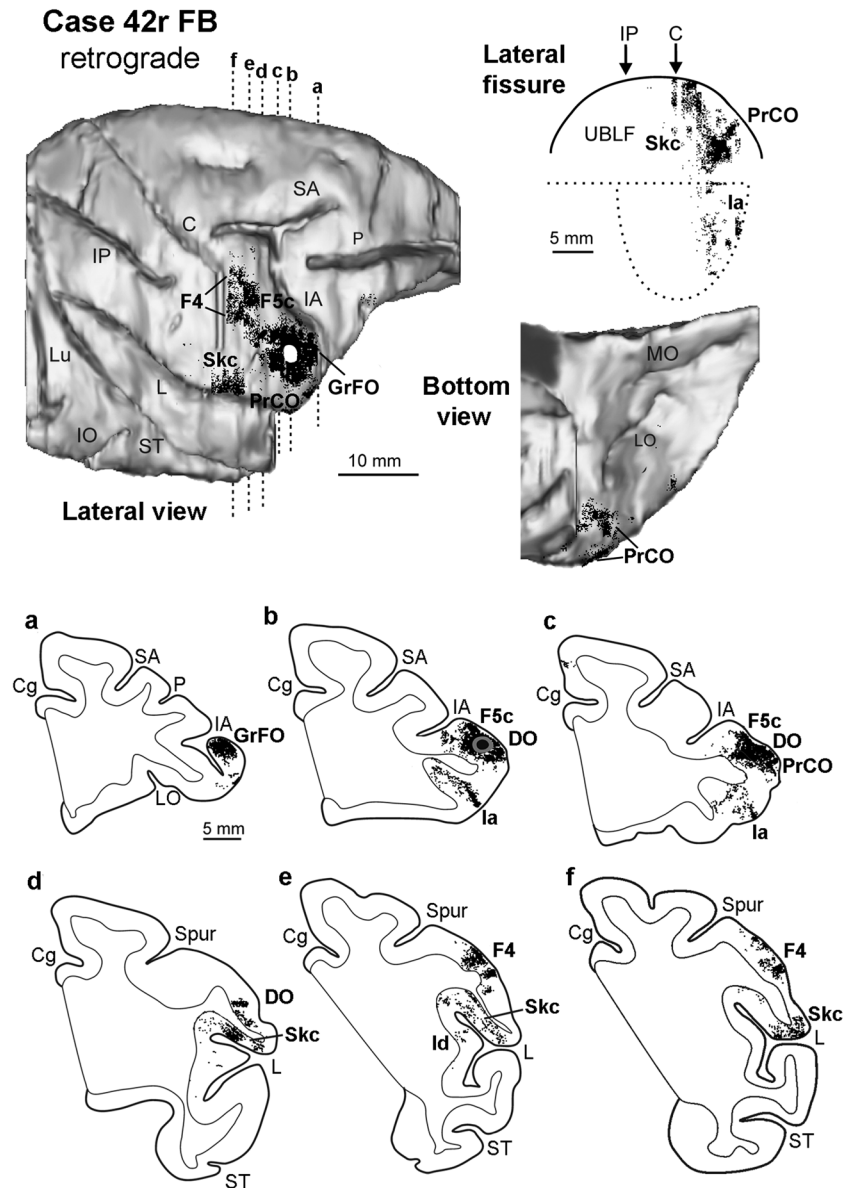
However, in both cases, the majority of marked cells was observed in the Bpc (Fig. 11). Finally, in Cases 331 CTBr and 42r FB (tracer injections in area DO), only very few, scattered cells were observed in the amygdala.

Discussion

The present study examined the connectivity of the recently defined architectonic area GrFO, located on the

opercular margin of the rostralmost part of the postarcuate cortex, and compared it with those of the two caudally adjacent opercular areas DO and PrCO. The results showed evidence for the connective distinctiveness of area GrFO, suggesting involvement of this area in the cortical network for controlling purposeful hand and face/mouth actions. Accordingly, the present data provide new insight into the organization of the macaque frontal opercular cortex, commonly considered as a whole involved in gustatory and oral sensory and motor functions.

Fig. 9 Distribution of the retrograde labeling observed after injections in area DO in Case 42r FB, shown in dorsolateral and bottom views of the 3D reconstructions of the injected hemisphere and in a 2D reconstruction of the LF (*upper part*), and in drawings of coronal sections arranged in a rostral to caudal order (*a–f lower part*). Abbreviations and conventions as in Figs. 1, 4, 5, and 6



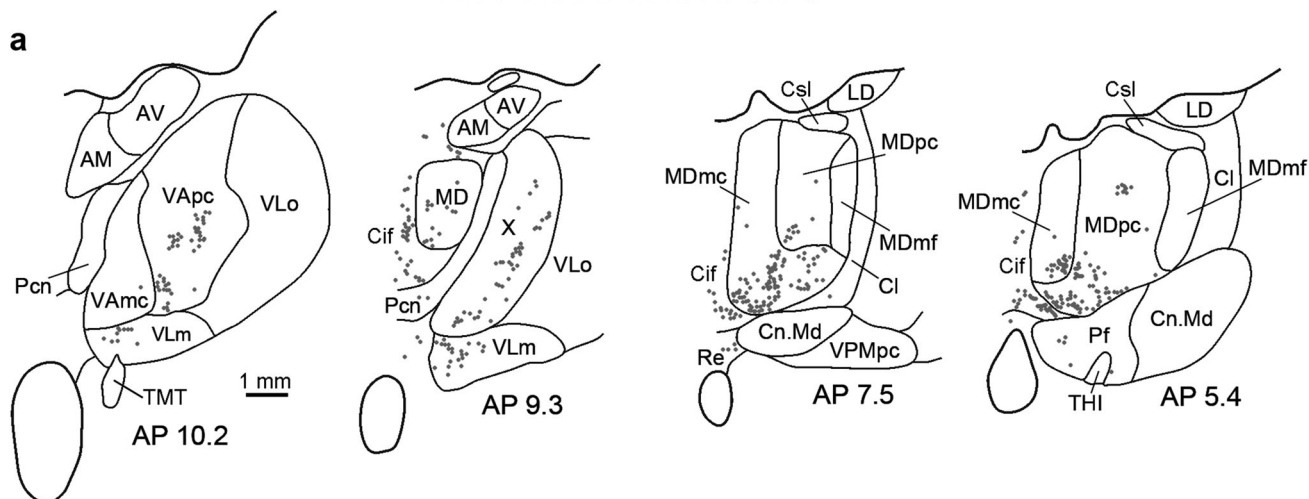
Connectional distinctiveness of area GrFO

The present data show that area GrFO is most strongly connected with areas F5a/44. GrFO also has strong connections with areas PrCO and DO, but has much weaker connections with areas F5c and F6/pre-SMA. Other frontal connections involve quite richly VLPF area 12l and orbitofrontal areas 12o, 12m, and 11, and more weakly VLPF areas 46v and 12r, and orbitofrontal area 13. Outside the frontal cortex, area GrFO is robustly connected with the agranular and dysgranular insula and with the agranular cingulate cortex and more weakly with area SII. Furthermore, area GrFO is the target of thalamic projections originating primarily from MDpc and intralaminar and midline nuclei, but also

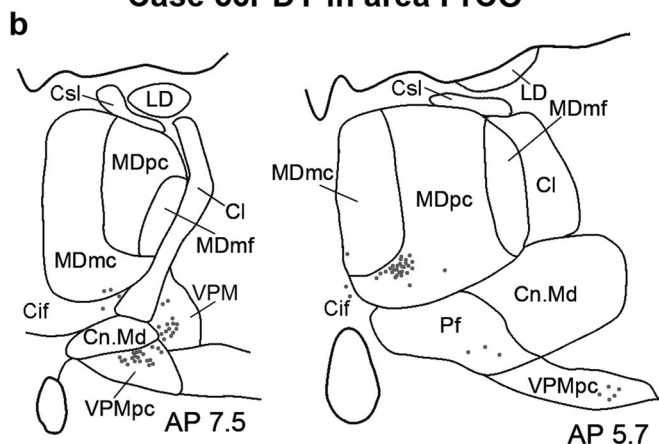
substantially from MDmc and motor thalamic nuclei VAPc and VLm, and of amygdalar projections mostly from the B nucleus.

The above-described connectivity pattern clearly distinguishes this area from the neighboring opercular, PMv, and prefrontal areas. First, areas PrCO and DO virtually lack connections with SII and are weakly connected to the cingulate cortex. Furthermore, area PrCO is robustly connected with areas G and Skc/SI and, compared to area GrFO, shows insular connections much stronger with the agranular than with the dysgranular sector, PMv connections much stronger with F5c than with F5a, and considerably weaker prefrontal connections. Robust projections from thalamic nuclei VPMpc and VPM further characterize area PrCO. Finally, the cortical connectivity almost

Case 61r FB in area GrFO



Case 56r DY in area PrCO



Case 42r FB in area DO

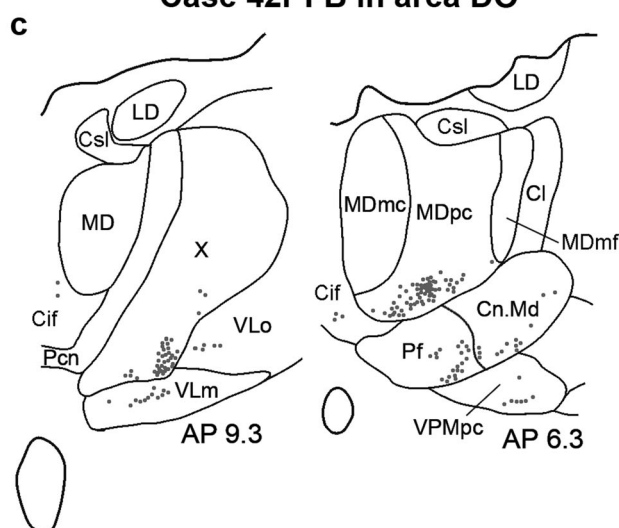


Fig. 10 Distribution of labeled thalamic neurons observed after injection in area GrFO in Case 61r FB (a), in area PrCO in Case 56r DY (b) and in area DO in Case 42r FB (c). The labeling is shown in drawings of coronal sections in rostral to caudal order selected at different AP levels according to the atlas of Olszewski (1952). Each dot corresponds to a single labeled neuron. AM anterior medial nucleus, AV anterior ventral nucleus, Cl central lateral nucleus, Cn.Md centromedian nucleus, Csl central superior lateral nucleus, LD lateral dorsal nucleus, MD mediadorsal nucleus, MDmc mediadorsal

nucleus, magnocellular part, MDmf mediadorsal nucleus, multiform part, MDpc mediadorsal nucleus, parvocellular part, Pcn paracentral nucleus, Pf parafascicular nucleus, Re reuniens nucleus, THI habenulointerpeduncular tract, TMT mammillothalamic tract, VAmc ventral anterior nucleus magnocellular part, VApC ventral anterior nucleus, parvocellular part, VLm ventral lateral nucleus, medial part, VLo ventral lateral nucleus, oral part, VPM ventral posterior medial nucleus, VPMpc ventral posterior medial nucleus, parvocellular part, X nucleus X of Olszewski (1952)

completely confined to the neighboring somatosensory and/or motor mouth-related areas Skc/SI, F4, F5c, and PrCO, the relatively robust input from motor thalamic nuclei, and the lack of amygdalar input distinguish area DO from area GrFO.

Second, differently from area GrFO, the two PMv areas F5a and F5c lack connections with orbitofrontal areas and are quite weakly connected with the insular cortex (Gerbella et al. 2011). Conversely, these two areas are

connected to different inferior parietal areas and display connections with SII much stronger than those of area GrFO. Furthermore, the rostral part of the PMv, as a whole, is characterized by thalamic projections primarily originating from area X (e.g., Schell and Strick 1984; Matelli et al. 1989).

Third, the two prefrontal areas 12l and 12o appear to differ from area GrFO for a very strong intraprefrontal connectivity and an extraprefrontal connectivity mostly

Table 3 Percent distribution (%), mean percent values (in bold), and total number (*n*) of thalamic-labeled neurons observed following retrograde tracer injections in areas GrFO, PrCO, and DO

Case	GrFO			PrCO			DO
	C56r FB (%)	C61r FB (%)	Mean (%)	C54l FB (%)	C56r DY (%)	Mean (%)	C42r FB (%)
Nucleus							
MD	1	2.5	1.7	–	–	–	*
MDmc	11.8	13.2	12.5	*	6.3	3.6	3
MDpc	38	31.7	34.8	28.5	39.5	34	34
MDdc	4.6	1.6	3.1	–	*	*	1
MDmf	–	*	*	–	–	–	1.2
VAmc	2.3	*	1.6	–	*	*	*
VApc	4.3	9.4	6.9	1.1	1.2	1.2	6.3
VLm	6.6	4.9	5.7	1.7	4.5	3.1	7.2
X	3.6	3.5	3.5	3.5	3	3.2	10
VLo	*	*	*	*	–	*	*
VPLo	–	*	*	2.2	–	1.1	3.6
VPM	*	–	*	8.5	5.7	7.1	*
VPMpc	1.7	–	*	15.4	24.3	19.8	2.1
VPI	1.1	–	*	–	2.1	1	–
Re	1.8	*	1.3	1.1	–	*	*
Clc-Cif- Cdc-Pac	11.2	20.2	15.7	12	3.3	7.6	4.7
Pcn-Cl	1.9	2.1	2	1.3	*	1	4.7
CnMd	2.1	1.1	1.6	16.8	2.7	9.7	13
Pf	2.9	2.5	2.7	4.1	3.6	3.8	3.8
Lim	1.5	1.4	1.4	–	–	–	*
SG	1.8	*	1	–	–	–	1.7
Pul.o	1	*	*	*	*	*	*
Pul.m	*	2.1	1.4	1.1	1.5	1.2	*
Total number ^a	3668	2423		459	334		1544

Cdc central densocellular nucleus, *Cif* central inferior nucleus, *Cl* central lateral nucleus, *Clc* central latocellular, *Cn.Md* centromedian nucleus, *Li* limitans nucleus, *MD* mediodorsal nucleus, *MDdc* mediodorsal nucleus, densocellular part, *MDmc* mediodorsal nucleus, magnocellular part, *MDmf* mediodorsal nucleus, multiform part, *MDpc* mediodorsal nucleus, parvicellular part, *Pcn* paracentral nucleus, *Pf* parafascicular nucleus, *Pul.m* pulvinar nucleus, medial part, *Pul.o* pulvinar nucleus, oral part, *Re* reuniens nucleus, *SG* suprageniculate nucleus, *VAmc* ventral anterior nucleus magnocellular part, *VApc* ventral anterior nucleus, parvicellular part, *VLm* ventral lateral nucleus, medial part, *VLo* ventral lateral nucleus, oral part, *VPI* ventral posterior inferior nucleus, *VPLo* ventral posterior lateral nucleus, oral part, *VPM* ventral posterior medial nucleus, *VPMpc* ventral posterior medial nucleus, parvicellular part, *X* Area X of Olszewski (1952)

– No labeling, * Labeling <1 %

^a Total number of thalamic-labeled cells plotted in sections at every 300- μ m interval

involving inferotemporal areas and the dysgranular insula (Carmichael and Price 1995; Saleem et al. 2014).

Very few studies have so far described the connectivity of the macaque frontal opercular cortex. Specifically, Cipolloni and Pandya (1999) placed relatively large tracer injections at different rostrocaudal levels of the opercular area designated as ProM, largely corresponding to area PrCO of Roberts and Akert (1963). The connectivity patterns observed by these authors after more caudal or more rostral injections, compared with the present data, appear quite compatible with an involvement primarily of our areas PrCO or GrFO, respectively. Furthermore, Simonyan and Jürgens (2002, 2005a) have described the

cortical connections of an opercular field, located at the border with the PMv, from which intracortical microstimulation (ICMS) evoked vocal fold movements (“laryngeal motor cortex”). The observed connectivity pattern was very extensive, including virtually all the areas that we found to be connected with areas GrFO, PrCO, and DO, and additional areas in which no labeling was observed in our study. However, it should be noted that the cortical field injected by Simonyan and Jürgens (2002, 2005a), though apparently corresponding mostly to the location of area DO, was defined as the zone common to several different injection sites that slightly varied in location across different animals and appeared to be

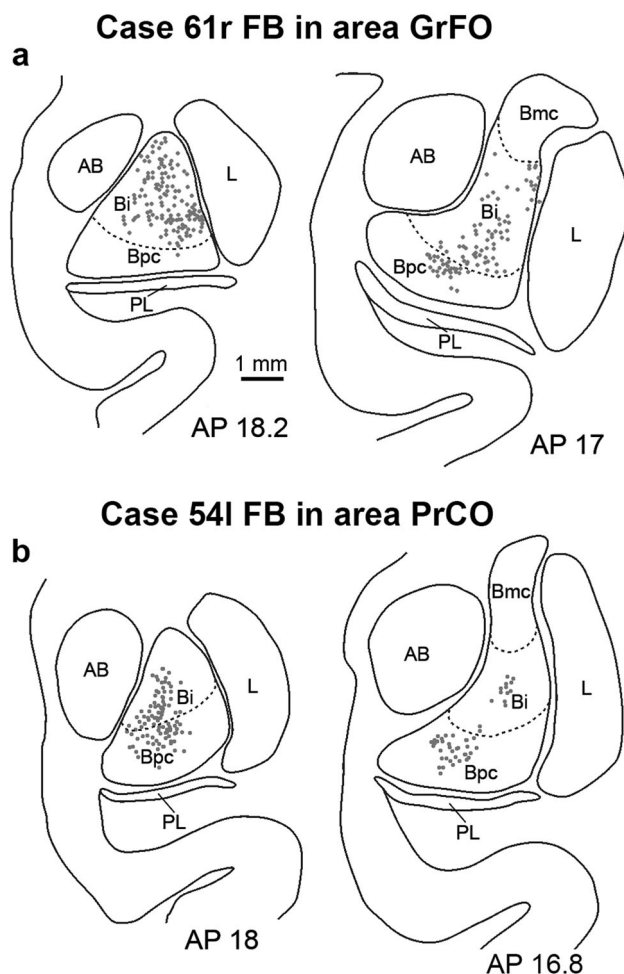


Fig. 11 Distribution of retrogradely labeled amygdalar neurons observed after injections in area GrFO in Case 61r FB (**a**) and in area PrCO in Case 54l FB (**b**). Each *dot* corresponds to one labeled neuron. For each case, the labeling is shown in two drawings of coronal sections, selected at different AP levels. The *dashed lines* mark the borders of the magnocellular, intermediate, and parvocellular subdivisions of the basal nucleus. *AB* accessory basal nucleus, *Bmc* magnocellular subdivision of the basal nucleus, *Bi* intermediate subdivision of the basal nucleus, *Bpc* parvocellular subdivision of the basal nucleus, *L* lateral nucleus, *PL* paralaminar nucleus

relatively large (about 5 mm in rostrocaudal extent in Simonyan and Jürgens 2005a). Accordingly, it is possible that the connectivity pattern described for the “laryngeal motor cortex” reflects, with some variability across different animals, involvement by the injection sites of all the three areas object of the present study and, possibly, of the adjacent PMv cortex. The described thalamic connectivity of the “laryngeal motor cortex” (Simonyan and Jürgens 2003, 2005b), characterized by extensive labeling in several different motor thalamic nuclei, MDpc, MDmc, and both VPM and VPMpc, is also compatible with involvement by the injection sites of at least areas DO and PrCO.

Functional considerations

The opercular frontal sector corresponding to area PrCO as defined by Roberts and Akert (1963) has been associated with gustatory functions and sensorimotor control of mouth, pharyngeal, and laryngeal movements (e.g., Ogawa 1994; Martin and Sessle 1993; Jürgens and Ehrenreich 2007). The connectivity patterns of areas PrCO and DO as defined in the present study likely represent the neural substrate for these proposed functions. Specifically, area PrCO displays robust connections with the opercular part of the Skc where sensory input from the oral cavity appears to be represented (Ogawa et al. 1989) and with the primary gustatory area G and is a target of VPMpc, the thalamic relay of the gustatory input to the cortex (e.g., Pritchard et al. 1986). These data are in agreement with an involvement of this area in the so-called “higher-order gustatory cortex” (Ogawa 1994). Furthermore, the rich connectivity of area DO with the ventralmost and the opercular parts of the Skc, where sensory input from face/mouth (Krubitzer et al. 1995) and from oral cavity (Ogawa et al. 1989) are represented, respectively, and with the ventral part of the caudal PMv area F4, is in line with data showing involvement of this field in oromotor functions. Indeed, Huang et al. (1989), in a study focused on the lateral part of the precentral cortex, observed that in a field likely involving also the location of area DO, intracortical microstimulation (ICMS) was effective in evoking rhythmic jaw movement, even using short train durations (35 ms). This field was referred to as “precentral cortical masticatory area” (CMAp). Furthermore, Martin et al. (1999) found that in this same field, ICMS with short train durations was also effective in evoking swallowing. Finally, the “laryngeal motor cortex” defined by Simonyan and Jürgens (2005b) appeared to largely involve the location of area DO, though also extending dorsally and rostrally. Considering the very long train durations (4 s) and high current intensities (up to 400 μ A) used in this study, it is possible that this zone was overestimated and actually is confined to area DO.

A different functional role is suggested by the present connective data for area GrFO. Differently from areas PrCO and DO, this area displays connections not only with mouth-, but also with hand-related fields. Specifically, area GrFO is connected to the SII hand representation (Fitzgerald et al. 2004), is very richly connected to the hand- and possibly face/mouth-related PMv area F5a (Fluet et al. 2010; Gerbella et al. 2011; Nelissen and Vanduffel 2011), and displays weaker connections with the hand- and face/mouth-related area F5c (Maranesi et al. 2012) and the arm-related area F6/pre-SMA (Luppino et al. 1991; Matsuzaka et al. 1992). Indeed, two electrophysiological studies focused on the ventral part of F5c, but also involving the

location of area GrFO, showed that in both these fields the majority of the recorded neurons was active during the execution of both hand and mouth actions (Ferrari et al. 2003, 2005). Furthermore, functional magnetic resonance imaging data showed that the cortical sector corresponding to area GrFO was activated during the execution of grasping in the dark (Nelissen and Vanduffel 2011). All together, these data suggest the involvement of area GrFO in the cortical circuits for controlling hand and face/mouth actions.

In this context, the strong connections with several cortical or subcortical structures affiliated to the limbic system markedly distinguish area GrFO from the adjacent PMv hand- and face/mouth-related areas and provide insight in the possible functional role of this area.

First, area GrFO is connected to the orbitofrontal cortex, a large, heterogeneous region considered to play a primary role in encoding the significance of stimuli within an emotional context and in the computation of good identities and subjective values in an abstract representation (Barbas 2007; Grabenhorst and Rolls 2011; Padoa-Schioppa and Cai 2011). Second, area GrFO is the target of projections from the amygdala, which could reach this area directly, or through thalamic relay in the MDmc (e.g., Russchen et al. 1987). The amygdala is a complex subcortical structure where sensory information originating mostly from higher-order sensory areas is endowed with emotional and motivational significance. Accordingly, this structure is an important node in emotion pathways and, through its efferent projections, is considered to play a crucial role in controlling appropriate emotional and behavioral responses to biologically relevant sensory stimuli (Barbas 2007). Third, area GrFO is richly and extensively connected to the agranular and the dysgranular insula. The primate insula is an anatomically and functionally heterogeneous integrative limbic region (Mesulam and Mufson 1982; Augustine 1996; Kurth et al. 2010), considered to play a fundamental and integrative role in the coordination between internal and external information through emotional subjective awareness (Ibañez et al. 2010). Based on functional and clinical evidence, it has been suggested that this region could be involved in a large variety of functions, including, for example, involvement in the basal subjective states that mediate action preparation (Ibañez et al. 2010) and evaluation of intentional action outcomes (Brass and Haggard 2010). Finally, area GrFO is connected to different subdivisions of the agranular cingulate area 24. Overall, the anterior cingulate cortex appears to play a crucial role in initiation, motivation, and goal-directed behaviors (Devinsky et al. 1995). Specifically, experimental evidence showed that cingulate motor areas could be involved in processing reward information for motor selection (Shima and Tanji 1998), in linking motivational outcomes to

behavior (Hayden and Platt 2010) and in integrating information about reward and errors in decision making (Chudasama et al. 2013).

Accordingly, the present data suggest that area GrFO is a site of integration of diverse types of limbic information which could be then conveyed mostly to the PMv area F5a. Connectional data showed that F5a is a privileged site of integration, in the PMv, of hand- and possibly face/mouth-related sensory-motor signals originating from inferior and opercular parietal areas with higher-order information originating from specific VLPF fields of areas 12r and 46v and from F6/pre-SMA (Gerbella et al. 2011). Based on these data, it was suggested that area F5a could play an important role in selecting and controlling goal-directed hand and possibly face/mouth actions based on actual or memory-based information on object features and information related to behavioral goals. The present data provide the neural substrate for a relatively direct contribution of limbic information related possibly to subjective values, emotional significance of stimuli, or internal states, to the selection of appropriate goal-directed actions. This contribution could be reflected in the modulation of observation-related activity of F5 mirror neurons by the value of the object grasped by another individual (Caggiano et al. 2012) and by the activity of F5 neurons related to the evaluation of the outcomes of behavioral choices (Pardo-Vazquez et al. 2008).

Acknowledgments The work was supported by Ministero dell'Istruzione, dell'Università e della Ricerca (grant number: PRIN 2010, 2010MEFNF7_005), European Commission Grant Cogsystems FP7-250013, and Interuniversity Attraction Poles (IAP) P7/11.

References

- Amaral D, Behniea H, Kelly J (2003) Topographic organization of projections from the amygdala to the visual cortex in the macaque monkey. *Neuroscience* 118:1099–1120
- Augustine JR (1996) Circuitry and functional aspects of the insular lobe in primates including humans. *Brain Res Brain Res Rev* 22:229–244
- Barbas H (2007) Specialized elements of orbitofrontal cortex in primates. *Ann NY Acad Sci* 1121:10–32
- Barbas H, Pandya DN (1987) Architecture and frontal cortical connections of the premotor cortex (area 6) in the rhesus monkey. *J Comp Neurol* 256:211–228
- Belmalih A, Borra E, Contini M, Gerbella M, Rozzi S, Luppino G (2009) Multimodal architectonic subdivision of the rostral part (area F5) of the macaque ventral premotor cortex. *J Comp Neurol* 512:183–217
- Bettio F, Demelio S, Gobetti E, Luppino G, Matelli M (2001) Interactive 3-D reconstruction and visualization of primates cerebral cortex. *Soc Neurosci Abstr Program No* 728:724
- Borra E, Gerbella M, Rozzi S, Luppino G (2011) Anatomical evidence for the involvement of the macaque ventrolateral prefrontal area 12r in controlling goal-directed actions. *J Neurosci* 31:12351–12363

- Brass M, Haggard P (2010) The hidden side of intentional action: the role of the anterior insular cortex. *Brain Struct Funct* 214:603–610
- Caggiano V, Fogassi L, Rizzolatti G, Casile A, Giese MA, Thier P (2012) Mirror neurons encode the subjective value of an observed action. *Proc Natl Acad Sci USA* 109:11848–11853
- Carmichael ST, Price JL (1994) Architectonic subdivision of the orbital and medial prefrontal cortex in the macaque monkey. *J Comp Neurol* 346:366–402
- Carmichael ST, Price JL (1995) Sensory and premotor connections of the orbital and medial prefrontal cortex of macaque monkeys. *J Comp Neurol* 363:642–664
- Chudasama Y, Daniels TE, Gorrin DP, Rhodes SE, Rudebeck PH, Murray EA (2013) The role of the anterior cingulate cortex in choices based on reward value and reward contingency. *Cereb Cortex* 23:2884–2898
- Cipolloni PB, Pandya DN (1999) Cortical connections of the frontoparietal opercular areas in the rhesus monkey. *J Comp Neurol* 403:431–458
- Devinsky O I, Morrell MJ, Vogt BA (1995) Contributions of anterior cingulate cortex to behaviour. *Brain* 118:279–306
- Felleman DJ, Van Essen DC (1991) Distributed hierarchical processing in primate cerebral cortex. *Cereb Cortex* 1:1–47
- Ferrari PF, Gallese V, Rizzolatti G, Fogassi L (2003) Mirror neurons responding to the observation of ingestive and communicative mouth actions in the monkey ventral premotor cortex. *Eur J Neurosci* 17:1703–1714
- Ferrari PF, Rozzi S, Fogassi L (2005) Mirror neurons responding to observation of actions made with tools in monkey ventral premotor cortex. *J Cogn Neurosci* 17:212–226
- Fitzgerald PJ, Lane JW, Thakur PH, Hsiao SS (2004) Receptive field properties of the macaque second somatosensory cortex: evidence for multiple functional representations. *J Neurosci* 24:11193–11204
- Fluet MC, Baumann MA, Scherberger H (2010) Context-specific grasp movement representation in macaque ventral premotor cortex. *J Neurosci* 30:15175–15184
- Gentilucci M, Fogassi L, Luppino G, Matelli M, Camarda R, Rizzolatti G (1988) Functional organization of inferior area 6 in the macaque monkey: I. Somatotopy and the control of proximal movements. *Exp Brain Res* 71:475–490
- Gerbella M, Belmalih A, Borra E, Rozzi S, Luppino G (2010) Cortical connections of the macaque caudal ventrolateral prefrontal areas 45A and 45B. *Cereb Cortex* 20:141–168
- Gerbella M, Belmalih A, Borra E, Rozzi S, Luppino G (2011) Cortical connections of the anterior (F5a) subdivision of the macaque ventral premotor area F5. *Brain Struct Funct* 216:43–65
- Gerbella M, Borra E, Rozzi S, Tonelli S, Luppino G (2012) Cortical connections of architectonically distinct areas of the Macaque frontal operculum. In: *Federation of European Neurosciences Societies Abstr Program No. 2806*
- Gerbella M, Borra E, Tonelli S, Rozzi S, Luppino G (2013) Connectional heterogeneity of the ventral part of the macaque area 46. *Cereb Cortex* 23:967–987
- Grabenhorst F, Rolls ET (2011) Value, pleasure and choice in the ventral prefrontal cortex. *Trends Cogn Sci* 15:56–67
- Hayden BY, Platt ML (2010) Neurons in anterior cingulate cortex multiplex information about reward and action. *J Neurosci* 30:3339–3346
- Huang CS, Hiraba H, Murray GM, Sessle BJ (1989) Topographical distribution and functional properties of cortically induced rhythmic jaw movements in the monkey (*Macaca fascicularis*). *J Neurophysiol* 61:635–650
- Ibañez A, Gleichgerrcht E, Manes F (2010) Clinical effects of insular damage in humans. *Brain Struct Funct* 214:397–410
- Jones EG, Burton H (1976) Areal differences in the laminar distribution of thalamic afferents in cortical fields of the insular, parietal and temporal regions of primates. *J Comp Neurol* 168:197–248
- Jürgens U, Ehrenreich L (2007) The descending motorcortical pathway to the laryngeal motoneurons in the squirrel monkey. *Brain Res* 1148:90–95
- Krubitzer L, Clarey J, Tweedale R, Elston G, Calford M (1995) A redefinition of somatosensory areas in the lateral sulcus of macaque monkeys. *J Neurosci* 15:3821–3839
- Kurth F, Zilles K, Fox PT, Laird AR, Eickhoff SB (2010) A link between the systems: functional differentiation and integration within the human insula revealed by meta-analysis. *Brain Struct Funct* 214:519–534
- Luppino G, Matelli M, Camarda RM, Gallese V, Rizzolatti G (1991) Multiple representations of body movements in mesial area 6 and the adjacent cingulate cortex: an intracortical microstimulation study in the macaque monkey. *J Comp Neurol* 311:463–482
- Luppino G, Rozzi S, Calzavara R, Matelli M (2003) Prefrontal and agranular cingulate projections to the dorsal premotor areas F2 and F7 in the macaque monkey. *Eur J Neurosci* 17:559–578
- Maranesi M, Rodà F, Bonini L, Rozzi S, Ferrari PF, Fogassi L, Coudé G (2012) Anatomic-functional organization of the ventral primary motor and premotor cortex in the macaque monkey. *Eur J Neurosci* 36:3376–3387
- Martin RE, Sessle BJ (1993) The role of the cerebral cortex in swallowing. *Dysphagia* 8:195–202
- Martin RE, Kempainen P, Masuda Y, Yao D, Murray GM, Sessle BJ (1999) Features of cortically evoked swallowing in the awake primate (*Macaca fascicularis*). *J Neurophysiol* 82:1529–1541
- Matelli M, Luppino G, Rizzolatti G (1985) Patterns of cytochrome oxidase activity in the frontal agranular cortex of macaque monkey. *Behav Brain Res* 18:125–137
- Matelli M, Luppino G, Fogassi L, Rizzolatti G (1989) Thalamic input to inferior area 6 and area 4 in the macaque monkey. *J Comp Neurol* 280:468–488
- Matelli M, Luppino G, Rizzolatti G (1991) Architecture of superior and mesial area 6 and of the adjacent cingulate cortex. *J Comp Neurol* 311:445–462
- Matelli M, Govoni P, Galletti C, Kutz DF, Luppino G (1998) Superior area 6 afferents from the superior parietal lobule in the macaque monkey. *J Comp Neurol* 402:327–352
- Matsuzaka Y, Aizawa H, Tanji J (1992) A motor area rostral to the supplementary motor area (presupplementary motor area) in the monkey: neuronal activity during a learned motor task. *J Neurophysiol* 68:653–662
- Mesulam MM, Mufson EJ (1982) Insula of the old world monkey. I. Architectonics in the insulo-orbito-temporal component of the paralimbic brain. *J Comp Neurol* 212:1–22
- Nelissen K, Vanduffel W (2011) Grasping-related functional magnetic resonance imaging brain responses in the macaque monkey. *J Neurosci* 31:8220–8229
- Ogawa H (1994) Gustatory cortex of primates: anatomy and physiology. *Neurosci Res* 20:1–13
- Ogawa H, Ito S, Nomura T (1989) Oral cavity representation at the frontal operculum of macaque monkeys. *Neurosci Res* 6:283–298
- Olszewski J (1952) *The thalamus of Macaca Mulatta*. S. Karger, New York
- Padoa-Schioppa C, Cai X (2011) The orbitofrontal cortex and the computation of subjective value: consolidated concepts and new perspectives. *Ann N Y Acad Sci* 1239:130–137
- Pardo-Vazquez JL, Leboran V, Acuna C (2008) Neural correlates of decisions and their outcomes in the ventral premotor cortex. *J Neurosci* 28:12396–12408

- Pritchard TC, Hamilton RB, Morse JR, Norgren R (1986) Projections of thalamic gustatory and lingual areas in the monkey, *Macaca fascicularis*. *J Comp Neurol* 244:213–228
- Roberts T, Akert K (1963) Insular and opercular cortex and its thalamic projections in *Macaca mulatta*. *Sweiz Archiv Neurol Neurochir Psychiatr* 92:1–43
- Rozzi S, Calzavara R, Belmalih A, Borra E, Gregoriou GG, Matelli M, Luppino G (2006) Cortical connections of the inferior parietal cortical convexity of the macaque monkey. *Cereb Cortex* 16:1389–1417
- Russchen FT, Amaral DG, Price JL (1987) The afferent input to the magnocellular division of the mediodorsal thalamic nucleus in the monkey *Macaca fascicularis*. *J Comp Neurol* 256:175–210
- Saleem KS, Miller B, Price JL (2014) Subdivisions and connectional networks of the lateral prefrontal cortex in the macaque monkey. *J Comp Neurol* 522:1641–1690
- Schell G, Strick PL (1984) The origin of thalamic inputs to the arcuate premotor and supplementary motor areas. *J Neurosci* 4:539–560
- Shima K, Tanji J (1998) Role for cingulate motor area cells in voluntary movement selection based on reward. *Science* 282:1335–1338
- Simonyan K, Jürgens U (2002) Cortico-cortical projections of the motorcortical larynx area in the rhesus monkey. *Brain Res* 949:23–31
- Simonyan K, Jürgens U (2003) Efferent subcortical projections of the laryngeal motorcortex in the rhesus monkey. *Brain Res* 974:43–45
- Simonyan K, Jürgens U (2005a) Afferent cortical connections of the motor cortical larynx area in the rhesus monkey. *Neuroscience* 130:133–149
- Simonyan K, Jürgens U (2005b) Afferent subcortical connections into the motor cortical larynx area in the rhesus monkey. *Neuroscience* 130:119–131